



Published in final edited form as:

Bioorg Med Chem Lett. 2014 June 1; 24(11): 2585–2588. doi:10.1016/j.bmcl.2014.03.033.

Discovery of Novel Bacterial Elongation Condensing Enzyme Inhibitors by Virtual Screening

Zhong Zheng^a, Joshua B. Parsons^b, Rajendra Tangallapally^a, Weixing Zhang^c, Charles O. Rock^b, and Richard E. Lee^{a,*}

^aDepartment of Chemical Biology and Therapeutics, St Jude Children's Research Hospital, Memphis, TN 38105, USA

^bDepartment of Infectious Diseases, St Jude Children's Research Hospital, Memphis, TN 38105, USA

^cDepartment of Structural Biology, St Jude Children's Research Hospital, Memphis, TN 38105, USA

Abstract

The elongation condensing enzymes in the bacterial fatty acid biosynthesis pathway represent desirable targets for the design of novel, broad-spectrum antimicrobial agents. A series of substituted benzoxazolinones was identified in this study as a novel class of elongation condensing enzyme (FabB and FabF) inhibitors using a two-step virtual screening approach. Structure activity relationships were developed around the benzoxazolinone scaffold showing that N-substituted benzoxazolinones were most active. The benzoxazolinone scaffold has high chemical tractability making this chemotype suitable for further development of bacterial fatty acid synthesis inhibitors.

Keywords

virtual screening; fatty acid synthesis; condensing enzymes; antibiotics

Bacterial fatty acid biosynthesis has emerged as an appealing target for the development of novel antibacterial chemotherapeutics.¹ Mammals utilize a single multifunctional enzyme complex that is structurally distinct from the dissociated bacterial system (FASII).² The catalytic steps are the same in both systems, but significant structural differences between the mammalian and bacterial system can be exploited to design specific inhibitors.^{1,2} Multiple inhibitors of the enoyl-acyl carrier protein (ACP) reductase step (FabI) have been described.³ For example, AFN-1252 is a nanomolar FabI inhibitor that eradicates

© 2014 Elsevier Ltd. All rights reserved.

*Corresponding author. Tel: +1 9015956617; fax: +1 9015955715. richard.lee@stjude.org.

Publisher's Disclaimer: This is a PDF file of an unedited manuscript that has been accepted for publication. As a service to our customers we are providing this early version of the manuscript. The manuscript will undergo copyediting, typesetting, and review of the resulting proof before it is published in its final citable form. Please note that during the production process errors may be discovered which could affect the content, and all legal disclaimers that apply to the journal pertain.

Supplementary data

Supplementary data associated with this article can be found in the online version

Staphylococcus aureus infections.^{4,5,6} However, FabI inhibitors are not broad spectrum agents because many important pathogens express structurally distinct enoyl-ACP reductases (FabK, FabL or FabV) that are refractory to FabI inhibitors.³ Our work is focused on the elongation condensing enzymes (3-ketoacyl-ACP synthase) because they are ubiquitously expressed in bacteria and the two subgroups (FabB and FabF) have superimposable active sites.⁷ These targets are essential in Gram-negative bacteria. Although this group of bacteria can incorporate extracellular fatty acids into phospholipid, FASII is required to produce the acyl chains in the lipopolysaccharide of the outer membrane.¹ Some Gram-positive bacteria (Streptococci) can circumvent FASII inhibitors by incorporating extracellular fatty acids, but others (Staphylococci) require FASII even when environmental fatty acids are present.⁸ The natural products cerulenin, thiolactomycin (TLM) and platensimycin target both FabB and FabF.^{9,10} These inhibitors are broad-spectrum agents with *in vivo* efficacy against Gram-positive and Gram-negative bacteria. However, they have severe limitations, including substandard pharmacokinetic properties and limited synthetic access.¹¹ New chemical scaffolds are clearly needed, and this paper describes a virtual screening approach to discover a novel class of elongation condensing enzyme inhibitors using *E. coli* FabB as the model.

The high resolution crystal structure of the FabB-TLM binary complex¹² was used as the template to identify the key pharmacophore features to be incorporated into the design of new condensing enzyme inhibitors. TLM binds non-covalently adjacent to the active site residue Cys163 (Fig. 1).¹² The carbonyl group forms hydrogen bonds with both His298 and His333 in the active site, and the isoprenoid moiety slides into a tight hydrophobic pocket sandwiched between Gly391/Phe392 and Ala271/Pro272. A standard molecular dynamics simulation using AMBER¹³ with a production run of 5 ns was carried out to gain a dynamic picture of TLM binding as well to optimize hydrogen positions. The chain A in the co-crystal structure of TLM bound to *E. coli* FabB (PDB: 2VB8)¹⁴ was used as the starting conformation. The complex system was solvated in explicit water molecules with counter ions to neutralize the system. Energy minimization was performed first with solute constrained then released. The system temperature was slowly heated from 0 to 300K followed by equilibration and production simulation. The observed binding mode of TLM in the crystal structure was highly stable and all key interactions were maintained through simulation. A free energy analysis was executed to provide residue-based energy contribution to the TLM binding (Fig. 2A).^{15, 16} This analysis showed that His298, Phe392, Thr302, Phe390, Val270, Pro272, Thr300, Gly391 and His333 contribute to TLM binding.

A two-step virtual screen was performed against *E. coli* FabB using a total of ≈ 1.1 million compounds from the Enamine (Advanced Collection) and Chembridge (EXPRESS-Pick Collection Stock and CORE Library Stock) libraries. A single-conformation UNITY¹⁷ database was created and 3D conformations were generated for each compound by Concord. Compound sets were filtered for a molecular weight cut off of 350 to search for lead-like inhibitors¹⁸ that allows for facile further modification. Using the key binding elements identified from MD simulation, a UNITY pharmacophore query was established including a hydrogen bond acceptor atom connected to a five-member ring that could form a bidentate interaction with His298 and His333 (Fig. 2B).¹⁹ Spatial constraints were applied to constrain

the three-dimensional conformation of pharmacophore features. This pharmacophore query search was applied to remove inactives and to simplify the subsequent computationally expensive docking step. Compounds that successfully passed the filter ($\approx 250,000$ compounds) were advanced into docking experiments using the Virtual Screening Workflow from Schrödinger.²⁰ Compounds were filtered to remove those with reactive functional groups. Compounds were docked with Glide HTVS followed by Glide SP.²¹ Preference was given in docking to compounds that could form the desired hydrogen bonds with His298 and His333. The top ranking 500 compounds were preserved for further examination. After consideration of binding pose by eye, chemical diversity and tractability, a total of 31 compounds were prioritized and acquired for *in vitro* testing (see Supplementary Fig. 1). TLM was incorporated in the virtual screening library from the beginning as a positive control. This compound passed the pharmacophore search filter and was ranked very high in the subsequent docking study.

The purchased compounds were all analyzed by LCMS to confirm purity and identity. All 31 compounds passed this step and were then screened using NMR wLOGSY assay²² to evaluate FabB binding (see Supplementary Fig. 1). The eight compounds that exhibited binding in the NMR wLOGSY assay were further tested as FabB inhibitors using the condensing enzyme radiochemical assay previously described¹² except myristoyl-ACP, which was substituted by lauryl-ACP synthesized using the *Vibrio harveyi* acyl-ACP synthetase enzyme.²³ Initial analysis of inhibition was conducted at a single final inhibitor concentration of 200 μM . Both screens revealed that compound **1** exhibited binding in NMR and showed 24% inhibition at 200 μM in the enzymatic assay. Dose response experiments established an IC_{50} of 800 μM (Table 1). The IC_{50} for compound **1** was confirmed by resynthesis and retesting in the enzyme assay.

A similarity search performed in SciFinder uncovered 11 analogues of compound **1** that were ordered and tested. The scifinder analysis was complemented by a medicinal chemistry effort to fill in the SAR through synthesis of 18 additional compounds. Compounds were synthesized in one step from appropriately substituted benzoxazolinones and structurally unique secondary amines using Mannich chemistry (Supplementary Scheme 1).²⁴ The inhibitory activities of compounds from both sets are listed and grouped by structure in Table 1.

Compared with the initial hit (**1**), many compounds in table 1 showed improved enzymatic inhibition at a single inhibitor concentration of 200 μM . Selected compounds were measured in dose response experiments producing IC_{50} values ranging from 235 – 625 μM (Table 1). Various benzoxazolinone substitutions were tested with R^1 and R^2 (5 and 6 position) halogen substitution producing the most potent analogs. It is notable that moving the chlorine atom from the 6 position in **1** to the 5 position in **6** substantially increased inhibitory activity. Most structural divergence in this series was introduced via R^3 N-substitution to the benzoxazolinone core, and divergent secondary and cyclic amines were used to probe for improved sidechain moieties in three subseries. First, a series of similar aliphatic amine side chains (**2–13**) were examined. Substituting tetrahydrofuran with a cyclopentyl ring in compounds **3** and **4** resulted in loss of activity. Tetrahydropyran system (**7** and **8**) was well tolerated as well as corresponding spiro-tetrahydropyran moieties (**10**

and **11**) which maintained inhibitory activity. Compound **11** had an IC₅₀ of 335 μM, on par with the best tetrahydrofuran analogue (**6**). The pyrrolidine ring in **13** was well tolerated in comparison with tetrahydrofuran compound **1**. In the second sub set (**14–22**), an aryl group was introduced into the side chain in place of the tetrahydrofuran group found in **1**. The most potent analog of this set was the simple phenyl compound **14** and **18** with a hydroxyl group on the meta-position. Replacing phenyl group with 2-pyridyl (**20**) and 3-pyridyl (**19**) groups did not improve potency. However, bioisosteric phenyl replacement of **14** with a thiophene ring (**21** and **22**) was well tolerated. The third subseries was designed to conformationally restrict the *ter*-amine side chain (set **23–30**) in which the benzyl group of compound **14** was attached by a 4- to 6-membered ring. Compounds **27** and **29** both with a 5-membered pyrrolidine ring and a bromo substitution on meta-position of the phenyl ring showed the best activity with IC₅₀'s of 260 μM and 253 μM, respectively. The cyclopropane group (**22**) was also a better substituent than methyl (**21**). Substituting 5-chloro of **27** with 5-cyano in **29**, or changing benzoxazole with benzothiazole **30** yielded comparable IC₅₀ values. The expectation that the benzoxazolinones would also be FabF inhibitors was tested by examining the IC₅₀ of compound **14** against FabF from *S. aureus*. The IC₅₀ of compound **14** against *E. coli* FabB was 235 μM compared to an IC₅₀ of 387 μM against *S. aureus* FabF, indicating the potential for broad-spectrum activity of this scaffold. (Fig. 3)

The docking of compound **14** into the TLM binding site (Fig. 1C) provides a rationale for understanding the structural basis of benzoxazolinones binding. The superimposition of compound **14** with TLM bound to the *E. coli* FabB enzyme showed that the ketone group on the oxazole ring mimics the bidentate binding mode with the catalytic His298 and His333, and the methylaniline group occupied the same binding pocket as the isoprene side chain of TLM forming favorable van der Waals interactions. Other active compounds were also modeled to study their potential binding conformations. Compound **6** and **27** adopted very similar poses to each other and **14** (Supplementary Fig. 2 A,B). They both formed two hydrogen bonds with His298 and His333. The respective cyclopropane (**6**) and pyrrolidine (**27**) side chains occupy the same cavity above H298 that was originally partially filled by the chiral 5-methyl group on thiophene ring in TLM, while the tetrahydrofuran (**6**) and bromobenzene (**27**) rings are located in the same binding pocket as the methylaniline group in **14**. Although an active inhibitor, compound **11** showed less favorable docking, as binding requires reorientation of the TLM binding site to fit the bigger azaspiro side chain, losing one hydrogen bond with His298 (Supplementary Fig. 2 C).

Compared to the FabB natural product inhibitors, the benzoxazolinones show selective inhibition of the condensing enzymes along with improved physicochemical properties and easy synthetic access. This new inhibitor class is being further explored to increase target affinity.

Supplementary Material

Refer to Web version on PubMed Central for supplementary material.

Acknowledgements

We would like to thank Laura Wells and Protein Production Shared Resource for their expert technical assistance. This study was supported by the National Institutes of Health grant 5R01GM034496, Cancer Center Support grant CA21765 and the American Lebanese Syrian Associated Charities (ALSAC).

References

1. Parsons JB, Rock CO. *Current opinion in microbiology*. 2011; 14:544. [PubMed: 21862391]
2. White SW, Zheng J, Zhang YM, Rock. *Annual review of biochemistry*. 2005; 74:791.
3. Lu H, Tonge PJ. *Acc Chem Res*. 2008; 41:11. [PubMed: 18193820]
4. Kaplan N, Albert M, Awrey D, Bardouniotis E, Berman J, Clarke T, Dorsey M, Hafkin B, Ramnauth J, Romanov V, Schmid MB, Thalakada R, Yethon J, Pauls HW. *Antimicrobial agents and chemotherapy*. 2012; 56:5865. [PubMed: 22948878]
5. Banevicius MA, Kaplan N, Hafkin B, Nicolau DP. *J Chemother*. 2013; 25:26. [PubMed: 23433441]
6. Yao J, Maxwell JB, Rock CO. *J Biol Chem*. 2013
7. Price AC, Rock CO, White SW. *J Bacteriol*. 2003; 185:4136. [PubMed: 12837788]
8. Parsons JB, Frank MW, Subramanian C, Saenkham P, Rock CO. *Proc Natl Acad Sci U S A*. 2011; 108:15378. [PubMed: 21876172]
9. Heath RJ, White SW, Rock CO. *Appl Microbiol Biotechnol*. 2002; 58:695. [PubMed: 12021787]
10. Parsons JB, Frank MW, Subramanian C, Saenkham P, Rock CO. *Proc Natl Acad Sci U S A*. 2011; 108:15378. [PubMed: 21876172]
11. Kim P, Zhang YM, Shenoy G, Nguyen QA, Boshoff HI, Manjunatha UH, Goodwin MB, Lonsdale J, Price AC, Miller DJ, Duncan K, White SW, Rock CO, Barry CE 3rd, Dowd CS. *J Med Chem*. 2006; 49:159. [PubMed: 16392800]
12. Price AC, Choi KH, Heath RJ, Li Z, White SW, Rock CO. *J Biol Chem*. 2001; 276:6551. [PubMed: 11050088]
13. Case, DA.; T. A. D.; Cheatham, TE., III; Simmerling, CL.; Wang, J.; Duke, RE.; Luo, R.; Walker, RC.; Zhang, W.; Merz, KM.; Roberts, BP.; Wang, B.; Hayik, S.; Roitberg, A.; Seabra, G.; Kolossvai, I.; Wong, KF.; Paesani, F.; Vanicek, J.; Liu, J.; Wu, X.; Brozell, SR.; Steinbrecher, T.; Gohlke, H.; Cai, Q.; Ye, X.; Wang, J.; Hsieh, M-J.; Cui, G.; Roe, DR.; Mathews, DH.; Seetin, MG.; Sagui, C.; Babin, V.; Luchko, T.; Gusarov, S.; Kovalenko, A.; Kollman, PA. University of California; San Francisco: 2010.
14. Pappenberger G, Schulz-Gasch T, Kusznir E, Muller F, Hennig M. *Acta Crystallogr D Biol Crystallogr*. 2007; 63:1208. [PubMed: 18084068]
15. Massova I, Kollman PA. *Perspect Drug Discov*. 2000; 18:113.
16. Zhu T, Lee H, Lei H, Jones C, Patel K, Johnson ME, Hevener KE. *J Chem Inf Model*. 2013; 53:560. [PubMed: 23432621]
17. Homer RW, Swanson J, Jilek RJ, Hurst T, Clark RD. *J Chem Inf Model*. 2008; 48:2294. [PubMed: 18998666]
18. Wunberg T, Hendrix M, Hillisch A, Lobell M, Meier H, Schmeck C, Wild H, Hinzen B. *Drug discovery today*. 2006; 11:175. [PubMed: 16533716]
19. Martin YC. *Journal of Medicinal Chemistry*. 1992; 35:2145. [PubMed: 1613742]
20. Schrodinger, LLC. New York, NY; 2013.
21. Repasky MP, Shelley M, Friesner RA. *Curr Protoc Bioinformatics*. 2007 Chapter 8, Unit 8 12.
22. Dalvit C, Fogliatto G, Stewart A, Veronesi M, Stockman B. *J Biomol NMR*. 2001; 21:349. [PubMed: 11824754]
23. Jiang Y, Chan CH, Cronan JE. *Biochemistry*. 2006; 45:10008. [PubMed: 16906759]
24. Gokhan N, Koksall M, Kupeli E, Yesilada E, Erdogan H. *Turk J Chem*. 2005; 29:445.

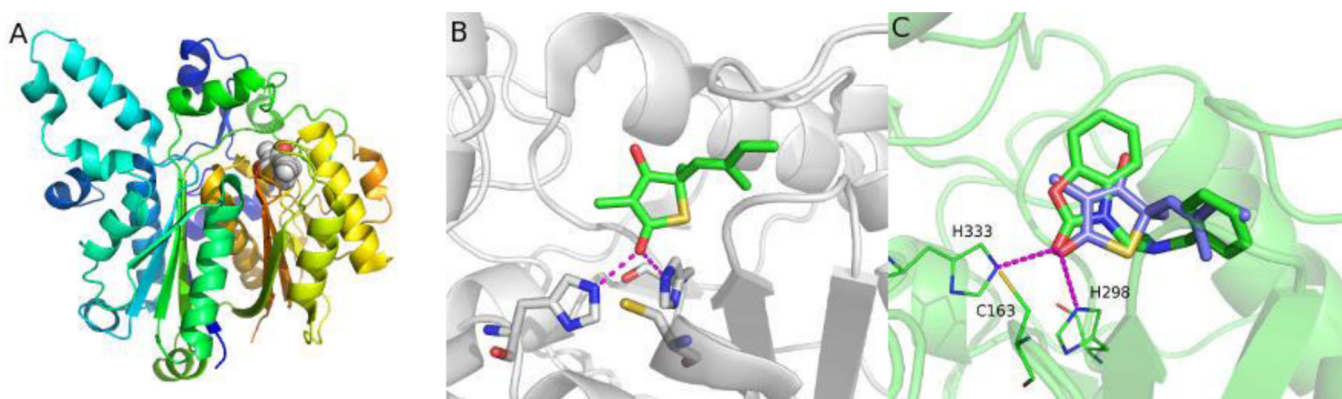


Figure 1. Binding modes of TLM and compound **14** to FabB. (A) Cocystal structure of TLM in complex with FabB from *E. coli* (PDB: 2vb8). TLM is shown in spheres. (B) A close-up view of the interactions between TLM and the binding site. (C) Compound **14** (green) docked into the binding site superimposed with TLM (purple).

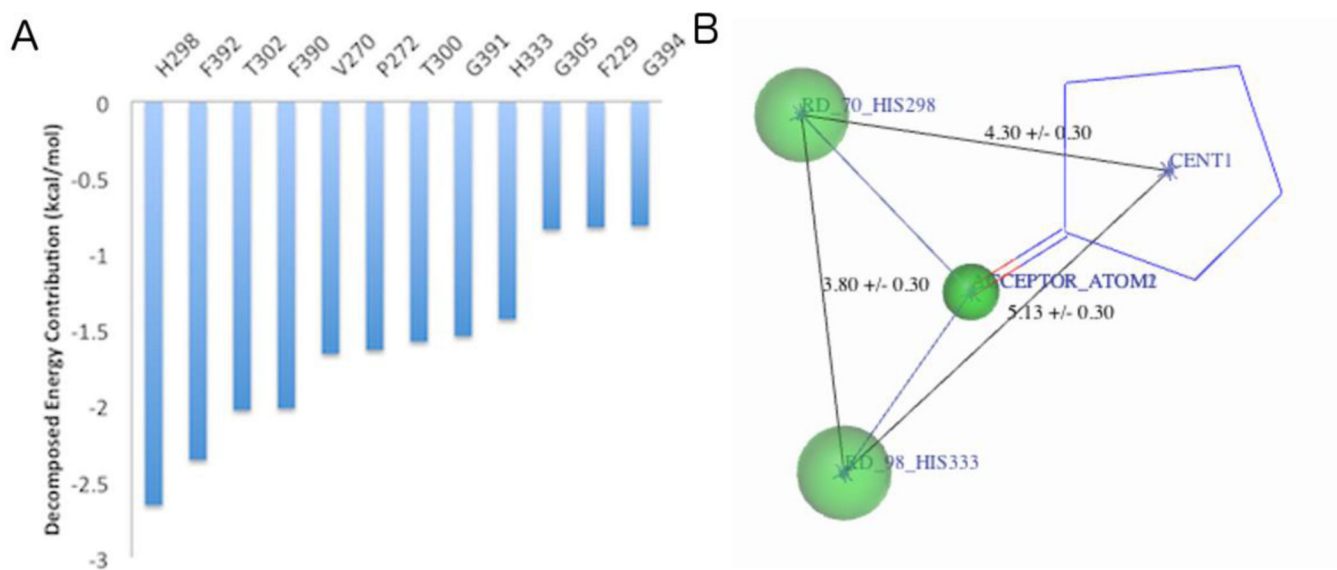


Figure 2. The TLM pharmacophore model. (A) Decomposed free energy contribution per residue to TLM binding calculated from MD simulation. (B) Pharmacophore model developed in UNITY.

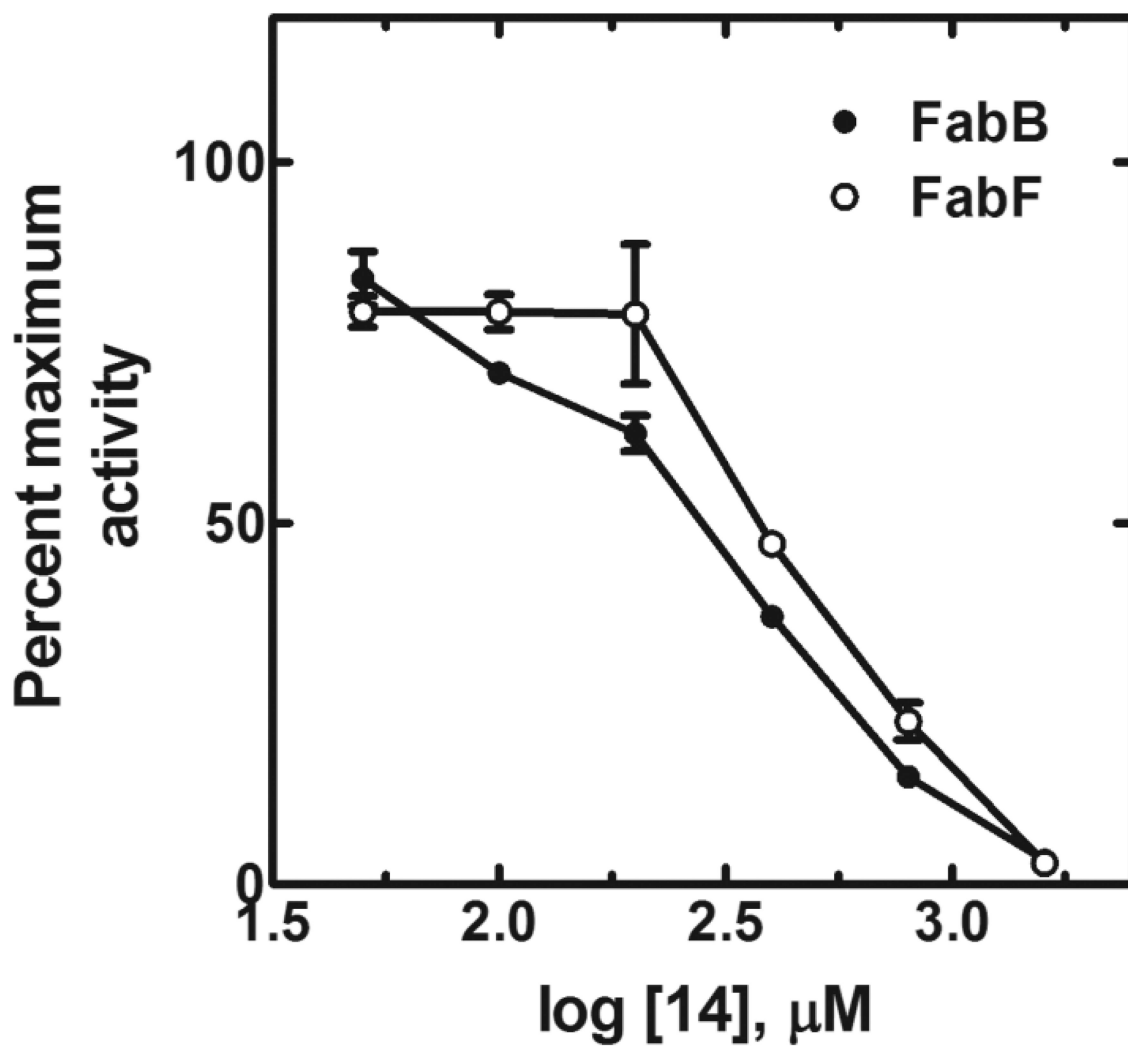


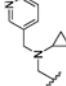
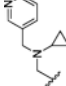
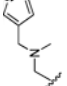
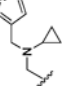
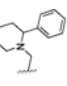
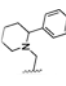
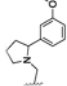
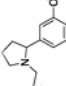
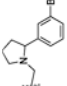
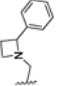
Figure 3. Compound **14** inhibition of *E. coli* FabB and *S. aureus* FabF *in vitro*. Maximum activities were: FabB, 4.7 nmoles/min/mg; FabF, 4.0 nmoles/min/mg.

The structures and measured FabB inhibition of compounds from procurement and chemical synthesis arranged for SAR purposes. All compounds with stereochemistry were tested as racemates.

Table 1

#	X	R ¹	R ²	R ³	%Inhibition @ 200 μ M	IC ₅₀ (μ M)
1	O	H	Cl		24.1	800
2	O	H	H		24	ND
3	O	Cl	H		17.7	ND
4	O	H	Br		17.7	ND
5	O	CH ₃	H		40.1	ND
6	O	Cl	H		36.7	350
7	O	H	Cl		31.7	ND
8	O	H	Cl		24.3	ND

#	X	R ¹	R ²	R ³	%Inhibition @ 200 μM	IC ₅₀ (μM)
9	O	H	Br		32.7	600
10	O	H	Cl		38.8	ND
11	O	Cl	H		37.7	335
12	O	H	Cl		26.4	ND
13	O	H	Cl		23.8	ND
14	O	H	H		33.5	235
15	O	H	Cl		32.1	ND
16	O	H	H		5	ND
17	O	H	Cl		28.3	ND
18	O	Cl	H		41.4	ND

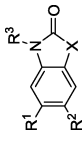
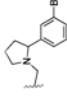
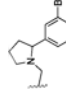
#	X	R ¹	R ²		R ³	%Inhibition @ 200 μM	IC ₅₀ (μM)
			R ¹	R ²			
19	O	H	Cl			23.6	ND
20	O	H	Cl			30	ND
21	O	H	H	H		30	ND
22	O	H	H	H		37.8	ND
23	O	H	Cl			38	ND
24	O	Cl	H			30.4	415
25	O	H	Cl			36.4	ND
26	O	Cl	H			37.1	305
27	O	Cl	H			55.4	260
28	O	Cl	H			31.9	ND

Author Manuscript

Author Manuscript

Author Manuscript

Author Manuscript

#	X	R ¹	R ²	R ³		%Inhibition @ 200 μM	IC ₅₀ (μM)
29	O	CN	H			42.1	253
30	S	Cl	H			36.1	303